Reaction Mechanism of N_2/H_2 Conversion to NH_3: A Theoretical Study

Der-Yan Hwang*,† and Alexander M. Mebel*,‡

Department of Chemistry, Tamkang University, Tamsui 25137, Taiwan, and Institute of Atomic and Molecular Sciences, Academia Sinica, P.O. Box 23-166, Taipei 10764, Taiwan

Received: September 20, 2002; In Final Form: January 9, 2003

Ab initio G2M(MP2)//MP2/6-31G** calculations have been performed to study the molecular and radical chain reaction mechanisms of nitrogen hydrogenation through sequential additions of three H_2 molecules to N_2 producing $NH_3 + NH_3$. All reaction steps of the molecular mechanism are shown to be slow owing to high barriers for the molecular hydrogen additions. The three-center 1,1-H_2 additions are significantly more preferable as compared to the four-center 1,2-additions. The most favorable reaction pathway involves the steps $N_2 + H_2 \rightarrow$ TS1a $\rightarrow NNH_2$, $NNH_2 + H_2 \rightarrow$ TS3a $\rightarrow H_2NNH_2$, $H_2NNH_2 \rightarrow$ TS4 $\rightarrow HNNH_3$, and $HNNH_3 + H_2 \rightarrow$ TS5 $\rightarrow NH_3 + NH_3$, with the barriers calculated as 125.2, 30.7, 60.5, and 24.6 kcal/mol, respectively. The addition of the first molecular hydrogen is thus the rate-determining stage of nitrogen hydrogenation. The formation of hydrazine can be facilitated by a spontaneous reaction of two *cis*-HNNH molecules by the dihydrogen transfer mechanism. The radical chain mechanism includes the $N_2 + H \rightarrow N_2H$, $N_2H + H_2 \rightarrow HNNH + H$, $HNNH + H \rightarrow N_2H_3$, $N_2H_3 + H_2 \rightarrow H_2NNH_2 + H$, $H_2NNH_2 + H \rightarrow NH_2 + NH_3$, and $NH_2 + H_2 \rightarrow NH_3 + H$ sequential reactions with the barriers of 17.1, 41.6, 6.4, 29.1, 10.7, and 10.6 kcal/mol, respectively. Nitrogen hydrogenation can be catalyzed by H atoms with the barrier for the slowest reaction step decreasing from 125 to 42 kcal/mol. The reaction of two $NH(^3\Sigma^-)$ radicals is predicted to be fast and to form $N_2 + H_2$ with high exothermicity. The reaction of two NH_2 radicals can produce $NNH_2 + H_2$ with exothermicity of 19.8 kcal/mol and a barrier of 10.9 kcal/mol relative to the reactants, or $NH_3 + NH(^3\Sigma^-)$, through a barrierless, 14.3 kcal/mol exothermic, but spin-forbidden channel. We also report rate constants and equilibrium constants for all considered reactions calculated using the transition state theory and ab initio energies and molecular parameters, which can be employed for kinetic modeling of chemical processes involving nitrogen- and hydrogen-containing substances.

1. Introduction

The hydrogenation of nitrogen molecule yielding ammonia is one of the most important processes of the chemical industry.[1] The heterogeneously catalyzed reaction was explored by Fritz Haber, who received the Nobel Prize in chemistry in 1918.[2] The search for more efficient catalysts is an active field of research, but only a little progress has been made since Mittasch suggested iron oxide catalysts, which are still in use today.[1] Moreover, up to now, more than eight decades after Haber's discovery, the complete mechanism of the uncatalyzed reaction $N_2 + 3H_2 \rightarrow 2NH_3$, which can be found in any general chemistry textbook, is still unknown. The fixation of N_2 and its reduction to NH_3 is also an important biological process, which takes place at the iron−molybdenum cofactor of the enzyme nitrogenase.[3,4] Hydrogen for the Haber process is more difficult to obtain compared to nitrogen. At present, the principal source is the reaction of petroleum products such as propane with steam in the presence of catalysts to produce hydrogen:

$$\underset{\text{steam}}{CH_3CH_2CH_3 + 6H_2O} \xrightarrow{\text{catalyst}} 3CO_2 + 10H_2$$

Hydrogen can also be prepared by the electrolysis of water and by the reaction of red-hot coal with steam. To improve the Haber process, a better understanding of the reaction mechanism for nitrogen hydrogenation is required.

The reaction of N_2 fixation and its reduction to NH_3 is thought to take place in three consecutive steps:

$$N_2 + H_2 \rightarrow N_2H_2$$

$$N_2H_2 + H_2 \rightarrow N_2H_4$$

$$N_2H_4 + H_2 \rightarrow 2NH_3$$

Although the energetics of these reactions is well-established experimentally and by high-level theoretical calculations,[5−10] except for the first reaction step,[7,8] little is known about the reaction mechanism and reaction barriers besides the fact that the barriers are high and the reactions do not occur without a catalyst even at elevated temperatures. The purpose of this study is to map out the entire reaction pathway of $N_2 + 3H_2 \rightarrow 2NH_3$ without a catalyst in order to establish the fundamental chemistry for further theoretical studies to improve the Haber process. The results of ab initio calculations reported in this paper include reliable structures of the reactants, products, intermediates, and transition states as well as their chemically accurate energies.

In addition, our results provide information on other reactions in the nitrogen/hydrogen system involving free radicals, including $N_2 + H$, $N_2H + H_2$, $N_2H_2 + H$, $N_2H_3 + H_2$, $N_2H_4 + H$, $NH + NH$, $NH_2 + NH_2$, and $NH + NH_3$, which are relevant to combustion and pyrolysis mechanisms of nitrogen-containing compounds, such as ammonia, to planetary atmosphere chem-

† Tamkang University.
‡ Academia Sinica.

10.1021/jp0270349 CCC: $25.00
Published on Web 04/01/2003

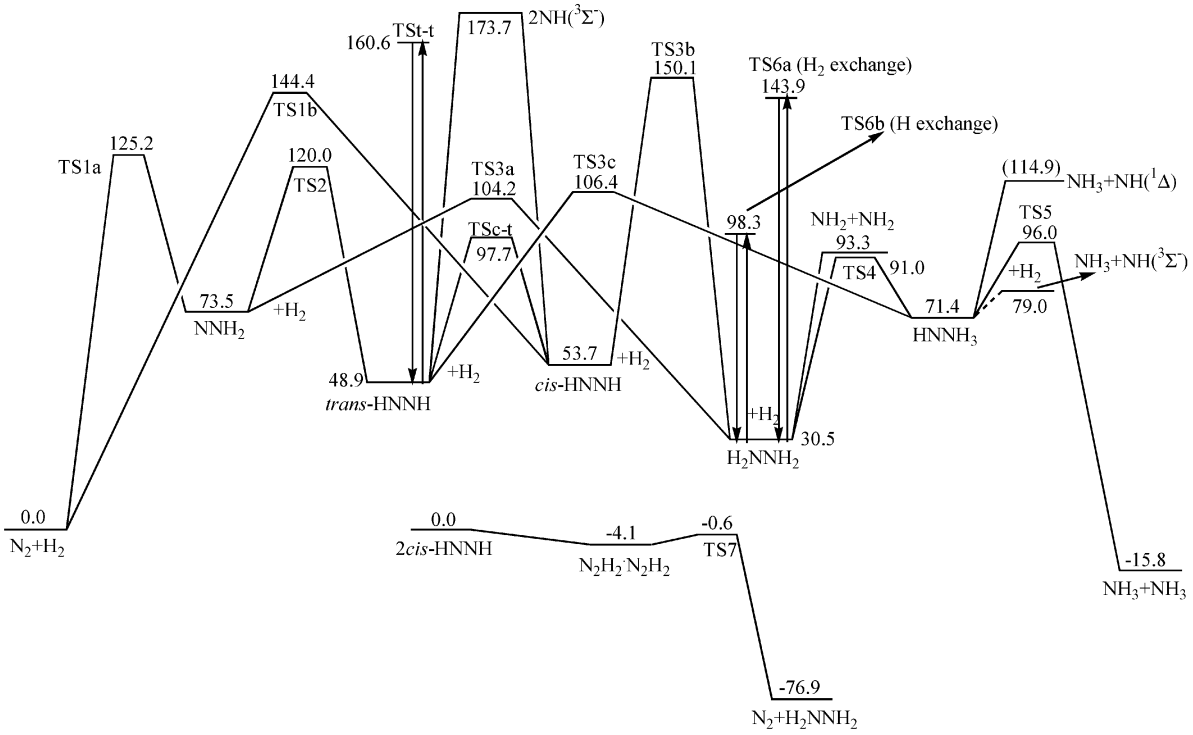

Figure 1. Potential energy diagram of various pathways in the molecular mechanism of the $N_2 + 3H_2 \rightarrow NH_3 + NH_3$ reaction calculated at the G2M(MP2)//MP2/6-31G** level of theory. All relative energies are given in kcal/mol.

istry, particularly those of Jupiter and Titan,[11] as well as to the NH_3 deNO_x[12] and the HNCO RAPRENO_x (rapid reduction of NO_x)[13] processes. Some of these reactions ($N_2 + H \rightarrow N_2H$ [14−17] and $N_2H_2 + H \rightarrow N_2H + H_2$ [18,19]) were studied earlier at various theoretical levels, but for most of them potential energy surfaces are investigated for the first time. We also carry out transition state theory (TST) calculations of rate constants and equilibrium constants for various reactions and report fitted rate expressions, which should be useful for kinetic modeling of chemical processes involving nitrogen- and hydrogen-containing substances.

2. Computational Details

Full geometry optimizations were run at the MP2/6-31G** level of theory[20] to locate various stationary points (reactants, intermediates, transition states, and products) on the ground singlet electronic state potential energy surface (PES) of the N_2/H_2 system. Harmonic vibrational frequencies were obtained at the MP2/6-31G** level in order to characterize the stationary points as minima (number of imaginary frequencies NIMAG = 0) or first-order saddle points (NIMAG = 1), to obtain zero-point vibrational energy corrections (ZPE) and to generate force constants needed for intrinsic reaction coordinate (IRC)[21] calculations. In order to predict more reliable ZPE, the raw calculated ZPE values were scaled by 0.967 to account for their average overestimation.[22] The IRC method[21] was used to track minimum energy paths from transition structures to the corresponding minimum. A step size of 0.1 amu$^{1/2}$ bohr or larger was used in the IRC procedure. The relative energies were refined using single-point calculations with MP2/6-31G** optimized geometry employing the G2M(MP2) method,[23] a modification of G2(MP2)[24] where QCISD(T)/6-311G** calculations are replaced by the coupled cluster[25] CCSD(T)/6-311G**. All the ab initio calculations described here were performed employing the Gaussian 98 program.[26]

3. Results and Discussion

ZPE-corrected relative energies of various species in the N_2/H_2 system calculated at the MP2/6-31G**, MP2/6-311G**, CCSD(T)/6-311G**, MP2/6-311+G(3df,2p), and G2M(MP2) levels of theory are listed in Table 1. Table 2 presents unscaled MP2/6-31G** calculated vibrational frequencies. The potential energy diagram along various reaction pathways involving closed-shell species computed at the G2M(MP2)//MP2/6-31G** level is shown in Figure 1. The optimized geometries of various compounds along these reaction pathways are depicted in Figure 2. Figure 3 shows potential energy diagrams for reactions with participation of free radicals, and Figure 4 presents the optimized geometries of corresponding reactants, products, and transition states.

3.1. $N_2 + H_2 \rightarrow N_2H_2$ Reaction. As seen in Figures 1 and 2, there are two possibilities for H_2 addition to the nitrogen molecule, to the same N atom (1,1-addition) and to two different nitrogens (1,2-addition). The 1,1-H_2 addition leads to the NNH_2 molecule via TS1a, and the 1,2-addition gives *cis*-HNNH via TS1b. Although the pathway leading to NNH_2 is much more endothermic than the one leading to *cis*-HNNH, TS1a lies 19.2 kcal/mol lower in energy than TS1b, so the 1,1-H_2 addition is significantly more favorable than the 1,2-addition. The calculated barrier for the $N_2 + H_2 \rightarrow NNH_2$ reaction is 125.2 kcal/mol. The structure of TS1a is peculiar, and the transition state can be characterized as late and asynchronous. One of the forming N−H bonds is already formed in the transition state with N−H distance of 1.009 Å, while the second N−H distance is as long as 1.776 Å and the H−H bond (1.525 Å) is practically broken. The second N−H bond starts to form only after TS1a is cleared. Our IRC calculations at the MP2/6-31G** level have confirmed that TS1a indeed connects the $N_2 + H_2$ reactants with NNH_2. The barrier for the 1,2-H_2 addition at TS1b is 144.4 kcal/mol, and this transition state exhibits a somewhat earlier and more synchronous character than TS1a. For instance, the

TABLE 1: ZPE Corrected Relative Energies (kcal/mol) Calculated at Different Levels of Theory for Various Species in the N_2/H_2 System

species	ZPE	MP2/6-31G** rel energy	MP2/6-311G** rel energy	CCSD(T)/6-311G** rel energy	MP2/6-311+G(3df,2p) rel energy	G2M(MP2) rel energy
$N_2 + H_2$[a]	9.70	0	0	0	0	0
TS1a	12.35	139.50	135.43	129.09	131.53	125.20
NNH_2	17.52	86.75	86.77	78.73	81.57	73.53
TS1b	10.56	158.57	155.60	146.94	153.08	144.43
TS1c	22.25	112.39	108.51	104.84	105.51	101.84
cis-HNNH	17.61	63.68	64.53	58.44	59.78	53.69
TSc-t	14.42	114.56	115.57	101.37	111.94	97.74
TSt-t	15.65	183.82	181.62	174.63	167.54	160.55
trans-HNNH	18.01	57.77	58.25	52.68	54.44	48.88 (48.8)[b]
TS2	13.80	134.06	133.45	126.28	127.12	119.95
NH + NH	9.74	174.54	176.00	162.85	180.46	173.71 (170.4)[c]
TS3a	26.94	119.96	118.47	110.64	112.03	104.21
TS3b	26.11	170.42	167.21	158.73	158.52	150.05
TS3c	28.11	122.98	120.09	112.26	114.24	106.41
H_2NNH_2	34.14	40.54	40.58	37.24	33.79	30.45 (26.3)[c]
TS4	30.50	107.55	106.40	101.90	95.48	90.98
$HNNH_3$	33.66	89.97	88.34	84.70	75.07	71.43
$NH_2 + NH_2$	24.77	102.75	103.57	94.35	99.29	93.28 (91.7)[c]
$NH_3 + NH$	27.12	85.75	85.89	78.60	83.04	78.97 (76.0)[c]
TS5	40.62	115.48	112.46	104.51	103.97	96.02
TS6a	37.30	154.78	149.60	151.77	141.71	143.88
TS6b	41.46	114.36	106.88	103.68	101.54	98.34
$NH_3 + NH_3$	44.50	−3.04	−4.23	−5.64	−14.37	−15.78 (−18.4)[c]
2 *cis*-HNNH	35.23	0	0	0	0	0
$N_2H_2 \cdot N_2H_2$	36.81	−5.60	−5.72	−5.28	−4.58	−4.13
TS7	36.27	−3.32	−4.15	−1.12	−3.62	−0.59
$N_2 + N_2H_4$	37.25	−86.82	−88.48	−79.64	−85.77	−76.93
$N_2 + H$	3.11	0	0	0	0	0
TS8	5.33	33.04	32.25	19.41	29.94	17.10
N_2H	9.98	27.66	28.20	15.24	24.37	11.42
$N_2H + H_2$	16.57	0	0	0	0	0
TS9	18.11	41.04	39.72	40.59	40.77	41.63
trans-HNNH + H	18.00	30.11	30.05	37.44	30.07	37.46
TS10	19.78	54.85	54.06	50.34	52.39	48.66
N_2H_3	25.68	−5.72	−5.89	−1.95	−8.83	−4.89
$N_2H_3 + H_2$	32.27	0	0	0	0	0
TS11	32.83	30.41	28.32	28.93	28.51	29.11
$N_2H_4 + H$	34.14	18.60	18.28	23.96	18.24	23.92
TS12	36.40	38.40	35.77	35.14	35.26	34.64
TS13	33.48	47.42	38.06	41.50	38.32	41.76
$NH_2 + NH_3$	34.63	−19.48	−19.84	−18.66	−21.08	−19.91

[a] Relative energies are given with respect to $N_2 + H_2$ for N_2H_2 species, $N_2 + 2H_2$ for N_2H_4, and $N_2 + 3H_2$ for N_2H_6. [b] In parentheses: experimental value from ref 35. [c] In parentheses: value obtained from experimental atomization energies given in refs 23 and 24.

H−H bond is stretched to 1.250 Å and two forming N−H bonds are 1.238 and 1.547 Å.

We have also investigated a possibility that the 1,1-H_2 addition could become more facile if it involves an additional H_2 molecule. The search of a transition state for the $N_2 + 2H_2 \rightarrow NNH_2 + H_2$ reaction resulted in TS1c. As seen in Figure 2, this transition state has a C_{2v}-symmetric structure and during the reaction the active N atom forms two new N−H bonds (1.278 Å in TS1c) with two hydrogens belonging to two different H_2 molecules, while a new molecular hydrogen is being formed from the other two H atoms; the corresponding H−H distance is 0.871 Å in the transition state. Two H−H bonds in the attacking H_2 molecules (1.165 Å in TS1c) are being broken. At the G2M level, TS1c resides 101.8 kcal/mol above $N_2 + 2H_2$, so the H_2 addition barrier is lowered by 23.4 kcal/mol as compared to that for the 1,1-H_2 addition via TS1a. However, despite this significant decrease, the barrier is still very high and the process is unlikely. Moreover, transition state TS1c corresponds to a reaction involving either a collision of three molecules or a two-body collision between a molecule (N_2) and a two-molecule complex (H_2 dimer). Three-particle collisions are very rare in the gas phase. The dimers of nonpolar molecules are weak: for instance, $(H_2)_2$ is bound by less than 0.1 kcal/mol[27] and cannot survive ambient temperatures. Therefore, clustering of H_2 molecules is not expected to assist nitrogen hydrogenation.

Three different isomers of the N_2H_2 species, *trans*-HNNH (48.9 kcal/mol above $N_2 + H_2$), *cis*-HNNH (53.7 kcal/mol), and NNH_2 (73.5 kcal/mol), can rearrange to each other. The $NNH_2 \rightarrow$ *trans*-HNNH isomerization occurs by a 1,2-H shift via TS2 with a barrier of 46.5 kcal/mol relative to NNH_2. In accordance with the fact that this reaction is exothermic, the transition state is rather early, with breaking and forming N−H bonds of 1.087 and 1.368 Å, respectively. The cis−trans rearrangement of HNNH takes place by rotation around the double N═N bond via TSc-t. The calculated barrier height, 44.0 and 48.8 kcal/mol relative to the cis and trans isomers, respectively, is typical for the rotation about a double bond. In addition, *trans*-HNNH can isomerize to itself by in-plane scrambling of the hydrogen atoms via TSt-t. However, the corresponding barrier, 111.7 kcal/mol, is very high and this process is not likely to occur.

TABLE 2: Vibrational Frequencies (cm^{-1}) of Various Compounds in the N_2/H_2 System Calculated at the MP2/6-31G Level of Theory**

species	frequencies
TS1a	2001i, 728, 792, 1261, 2136, 3725
NNH_2	1060, 1364, 1664, 1783, 3173, 3211
TS1b	3234i, 850, 1041, 1303, 1743, 2447
TS1c	2036i, 319, 570, 896, 1248, 1306, 1327, 1430, 1609, 1890, 2273, 2698
cis-HNNH	1287, 1373, 1562, 1567, 3225, 3306
TSc-t	1328i, 964, 1117, 1306, 3341, 3357
TSt-t	2148i, 280, 805, 1748, 4028, 4088
trans-HNNH	1349, 1360, 1525, 1628, 3353, 3382
TS2	2423i, 636, 1359, 1541, 2918, 3203
TS3a	1678i, 327, 630, 912, 1092, 1290, 1343, 1422, 1741, 2897, 3533, 3656
TS3b	2421i, 442, 866, 943, 1111, 1257, 1347, 1412, 1525, 2557, 3376, 3430
TS3c	1052i, 712, 775, 842, 1131, 1204, 1395, 1524, 1688, 3285, 3467, 3640
H_2NNH_2	180, 978, 1095, 1128, 1292, 1514, 1670, 1728, 3516, 3534, 3613, 3632
TS4	1467i, 260, 736, 926, 966, 1406, 1546, 1612, 3023, 3483, 3627, 3756
$HNNH_3$	448, 834, 1030, 1073, 1510, 1522, 1691, 1721, 3306, 3344, 3469, 3601
TS5	1172i, 62, 144, 447, 450, 548, 690, 802, 1150, 1151, 1411, 1694, 1709, 3489, 3556, 3651, 3717, 3743
TS6b	1725i, 217, 255, 697, 850, 941, 1078, 1228, 1326, 1428, 1564, 1688, 1706, 2463, 2856, 3455, 3565, 3684
$N_2H_2 \cdot N_2H_2$	54, 73, 132, 134, 164, 338, 1284, 1322, 1369, 1409, 1556, 1561, 1567, 1588, 3265, 3284, 3317, 3332
TS7	298i, 198, 320, 409, 477, 735, 1212, 1287, 1323, 1362, 1461, 1539, 1563, 1623, 2457, 2809, 3265, 3331
TS8	2276i, 796, 2918
N_2H	1050, 2895, 3015
TS9	2431i, 448, 644, 1246, 1381, 1474, 1509, 2601, 3367
TS10	1622i, 488, 581, 1327, 1408, 1572, 1848, 3271, 3338
N_2H_3	633, 761, 1170, 1297, 1518, 1712, 3527, 3590, 3754
TS11	2456i, 230, 439, 674, 878, 1095, 1180, 1280, 1434, 1550, 1659, 1714, 3533, 3591, 3710
TS12	2023i, 284, 677, 742, 1066, 1130, 1154, 1398, 1414, 1603, 1669, 3521, 3537, 3627, 3642
TS13	2292i, 56, 546, 959, 1044, 1150, 1203, 1339, 1407, 1465, 1610, 2172, 3430, 3487, 3550

Since the N_2H_2 system has been well studied by various theoretical methods,[5−8,20,28−33] we can compare our results with the results of previous calculations. The G2(MP2)//MP2/6-31G** relative energies of various N_2H_2 species with respect to the most stable *trans*-HNNH isomer are the following: 4.8 kcal/mol for *cis*-HNNH, 24.7 kcal/mol for NNH_2, 48.9 kcal/mol for TSc-t, and 71.1 kcal/mol for TS2; they are in close agreement with earlier G2 values of 5, 24, 50, and 70 kcal/mol, respectively.[7] For TS1a, the MP4/6-311G(2d,p) literature value of 82 kcal/mol [8] overestimates our G2M(MP2) result by 5.7 kcal/mol.

We can also look at the reaction of two imino $NH(^3\Sigma^-)$ radicals. They can recombine with each other, producing cis and trans isomers of diazene with calculated energy gains of 120.0 and 124.8 kcal/mol, respectively. The energized HNNH molecules can easily overcome the isomerization barriers at TSc-t and TS2 and dissociate to $N_2 + H_2$ via TS1a or even TS1b: both lie significantly lower in energy than the $NH(^3\Sigma^-) + NH(^3\Sigma^-)$ reactants. Therefore, the $NH(^3\Sigma^-) + NH(^3\Sigma^-)$ reaction is expected to produce molecular nitrogen and hydrogen. The calculated heat of this reaction, 173.7 kcal/mol, overestimates the experimental value[34] by 3.3 kcal/mol (see Table 1). On the other hand, the experimental endothermicity of the $N_2 + H_2 \rightarrow$ *trans*-HNNH reaction, 48.8 ± 0.5 kcal/mol,[35] is closely reproduced by our G2M(MP2) calculations.

3.2. $N_2H_2 + H_2 \rightarrow N_2H_4$ Reaction. Hydrogen addition to diazene can occur by three different pathways. The most favorable one is the 1,1-H_2 addition to NNH_2 yielding H_2NNH_2 via TS3a with a barrier of 30.7 kcal/mol relative to $NNH_2 + H_2$. The reaction is calculated to be 43.0 kcal/mol exothermic and the transition state exhibits an early character. For instance, the H−H bond in TS3a is stretched only by 0.130 Å compared to that for isolated H_2 at the same MP2/6-31G** level of theory and the forming N−H bonds are still long, 1.297 and 1.569 Å (see Figure 2). The 1,2-H_2 addition to *cis*-diazene occurs via TS3b and depicts a much higher barrier of 96.4 kcal/mol. Judging from the length of the breaking H−H bond, 1.168 Å in TS3b, this transition state has a later character than TS3a. The heat of the $N_2H_2 + H_2 \rightarrow N_2H_4$ reaction computed at the G2M(MP2) level with regard to the most stable isomer of diazene, *trans*-HNNH, −18.4 kcal/mol, is underestimated as compared to the experimental value of −22.5 kcal/mol.[34] Finally, the 1,1-H_2 addition to *trans*-diazene can produce another isomer of the N_2H_4 species, $HNNH_3$, via transition state TS3c. The barrier for this pathway is calculated as 57.5 kcal/mol relative to *trans*-HNNH + H_2, and TS3c resides 106.4 kcal/mol higher in energy than $N_2 + 2H_2$. The structure of TS3c is rather similar to that of TS1a, with one short (1.040 Å) and one long (1.785 Å) forming N−H bonds. The H−H bond, which is broken during the reaction, is stretched to 1.385 Å in the transition state. On the other hand, the H−H bond length is shorter than that in TS1a, 1.525 Å, indicating an earlier character of TS3c compared to TS1a. This result is in line with lower endothermicity of the *trans*-HNNH + $H_2 \rightarrow HNNH_3$ reaction, only 22.5 kcal/mol vs 73.5 kcal/mol for $N_2 + H_2$.

3.3. Isomerization of N_2H_4 and $N_2H_4 + H_2 \rightarrow 2NH_3$ Reaction. The last step of nitrogen hydrogenation is the addition of a third H_2 molecule to N_2H_4. Only the 1,1-H_2 addition can take place, but before this process can occur one of the hydrogen atoms has to be moved from one NH_2 group in hydrazine to another, thus releasing some room for the H_2 molecule to attack. Indeed, we were able to find, in addition to H_2NNH_2, another isomer of the N_2H_4 species, nitrene, $HNNH_3$, which is destined to play a key role in the last step of nitrogen hydrogenation. $HNNH_3$ resides 40.9 kcal/mol higher in energy than hydrazine and can be obtained from the latter by the 1,2-H migration. This process takes place via TS4 with a 60.5 kcal/mol barrier. The transition state for this endothermic rearrangement develops late, as the breaking N−H bond in TS4 is as long as 1.449 Å and the newly forming N−H bond, 1.069 Å, is only ~5% longer than the N−H bond in the product. According to our calculations, $HNNH_3$ is only 7.6 kcal/mol more stable than $NH_3 + NH(^3\Sigma^-)$. However, decomposition of $HNNH_3$ to these products is spin-forbidden. The lowest singlet state of the imino radical, $NH(a^1\Delta)$, lies 35.9 kcal/mol higher in energy than the $X^3\Sigma^-$ ground triplet state.[36] Based on this, the N−N bond strength in

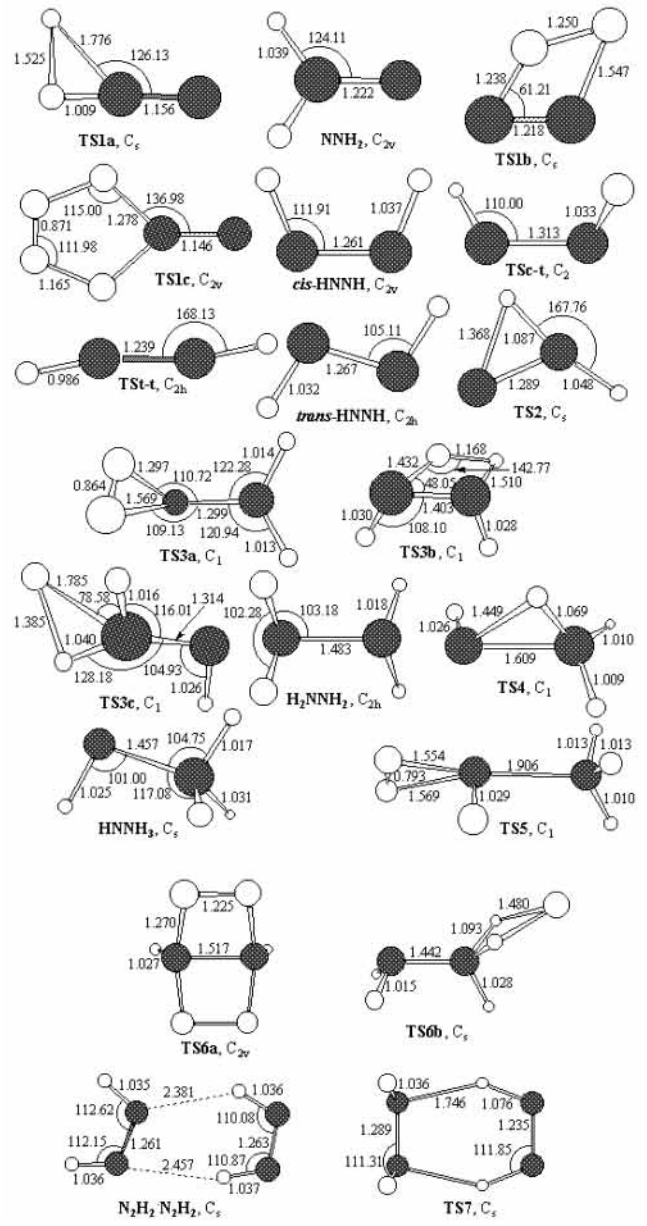

Figure 2. MP2/6-31G** optimized geometries of various species in the molecular mechanism of the $N_2 + 3H_2 \rightarrow NH_3 + NH_3$ reaction. Bond lengths are in angstroms and bond angles are in degrees.

$HNNH_3$ can be evaluated as 43.5 kcal/mol. This fact and the fact that the reverse barrier for the 1,2-H shift to form hydrazine is 19.6 kcal/mol make nitrene a quite stable intermediate. The electronic structure of nitrene can be described in terms of a zwitterionic $HN^- - N^+H_3$ electronic configuration.

Next, the $HNNH_3 + H_2 \rightarrow 2NH_3$ reaction can occur via TS5 with a barrier of 24.6 kcal/mol (65.5 kcal/mol relative to hydrazine). The reaction combines the H_2 addition with a rupture of the N−N bond. The transition state TS5 can be characterized as asynchronous, rather late with respect to the N−N bond rupture (the N−N bond is elongated by ∼31% to 1.906 Å) but very early with regard to the cleavage of the H−H bond (0.793 Å) and formation of two N−H bonds (1.554 and 1.569 Å). Relative to hydrazine, the calculated G2(MP2)//MP2/6-31G** exothermicity of the $N_2H_4 + H_2 \rightarrow NH_3 + NH_3$ reaction is 46.2 kcal/mol, fairly close to the experimental value of 44.7 kcal/mol.[34]

We also tried to find a pathway for the 1,2-H_2 addition to H_2NNH_2, but the search for a 1,2-addition transition state appeared to be unsuccessful, indicating that this process cannot occur. Instead, we found two transition states for molecular and atomic hydrogen exchanges, $H_2NNH_2 + H_2 \rightarrow H_2NNH_2 + H_2$. In the C_{2v}-symmetric TS6a, one hydrogen molecule attacks hydrazine but another one is leaving, so the reactants and products are formally the same. In TS6b, the attacking H_2 exchanges one of its H atoms with a hydrazine's hydrogen. The calculated barriers at TS6a and TS6b are high, 67.8 and 113.4 kcal/mol relative to hydrazine, respectively, and the exchange processes are not expected to be significant.

TABLE 3: Relative Energies (kcal/mol) of N_2H_4 Isomers and Transition State Calculated at the Coupled Cluster CSSD(T) and Multireference Full Valence Active Space[a] CASSCF and MRCI Levels of Theory with the 6-311G Basis Set[b]**

	CASSCF	MRCI	MRCI + Q[c]	CCSD(T)
H_2NNH_2	0	0	0	0
$HNNH_3$	45.53	46.28	46.13	47.46
TS4	64.56	63.57	63.04	64.66

[a] Fourteen electrons distributed on twelve orbitals, (14,12). [b] ZPE corrections obtained at the MP2/6-31G** level and scaled by 0.967 are included. [c] With Davidson corrections for quadruple excitations.

In order to verify the accuracy of our G2M(MP2) energies, especially for nonclassical or zwitterionic ($HNNH_3$) structures, we carried out multireference CASSCF[37] and internally contracted MRCI[38] calculations of two N_2H_4 isomers and the transition state TS4 between them using the MOLPRO 2000 program.[39] These calculations were performed with the full valence active space including 14 electrons distributed on 12 orbitals and with the 6-311G** basis set. The results are shown in Table 3 and can be compared with the CCSD(T)/6-311G** values. As one can see, the relative energies of $HNNH_3$ and TS4 with respect to H_2NNH_2 obtained at the CASSCF and MRCI levels do not deviate from the CCSD(T) energies by more than 1−2 kcal/mol. Therefore, the energies calculated at the G2M(MP2) level emulating the CCSD(T)/6-311+G(3df,2p) approach are expected to be reliable.

Overall, the most favorable reaction pathway for sequential hydrogenation of N_2 by three hydrogen molecules is the following:

$$N_2 + H_2 \rightarrow TS1a \rightarrow NNH_2$$

$$NNH_2 + H_2 \rightarrow TS3a \rightarrow H_2NNH_2$$

$$H_2NNH_2 \rightarrow TS4 \rightarrow HNNH_3$$

$$HNNH_3 + H_2 \rightarrow TS5 \rightarrow NH_3 + NH_3$$

The calculated barriers for the four steps are 125.2, 30.7, 60.5, and 24.6 kcal/mol, respectively. Considering the most stable isomers of the N_2H_2 and N_2H_4 species, the barriers for H_2 addition to these molecules are 55.3 and 65.5 kcal/mol and *trans*-HNNH requires initial isomerization to NNH_2 via a higher barrier of 71.1 kcal/mol. Starting from diazene, the most favorable reaction pathway is the following:

$$\textit{trans}\text{-HNNH} + H_2 \rightarrow TS3c \rightarrow HNNH_3$$

$$HNNH_3 + H_2 \rightarrow TS5 \rightarrow NH_3 + NH_3$$

and the higher barrier of 57.5 kcal/mol is calculated for the first step. The addition of the first hydrogen molecule to N_2 is clearly the slowest and rate-determining stage of nitrogen hydrogenation

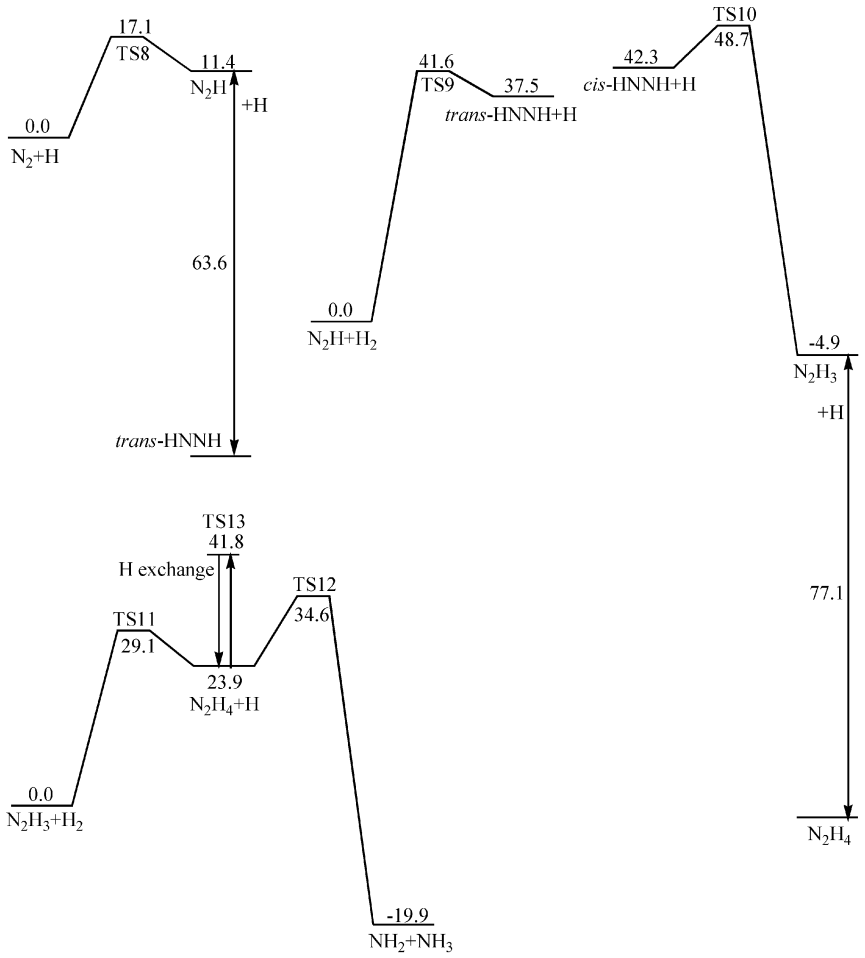

Figure 3. Potential energy diagram of various pathways in the radical chain mechanism of the $N_2 + 3H_2 \rightarrow NH_3 + NH_3$ reaction calculated at the G2M(MP2)//MP2/6-31G** level of theory. All relative energies are given in kcal/mol.

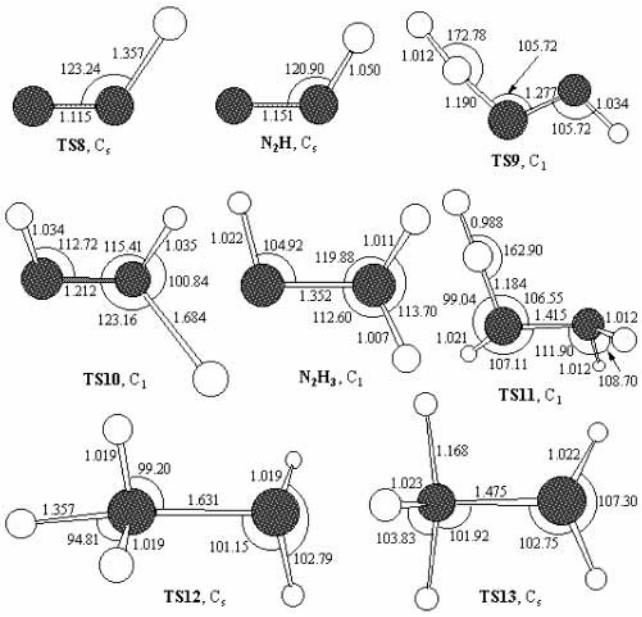

Figure 4. MP2/6-31G** optimized geometries of various species in the radical chain mechanism of the $N_2 + 3H_2 \rightarrow NH_3 + NH_3$ reaction. Bond lengths are in angstroms and bond angles are in degrees.

and a catalytic enhancement of the $N_2 + H_2 \rightarrow N_2H_2$ reaction is the most critical.

Let us now consider the reaction of two amino radicals, NH_2-($^2B_1$). The calculated N−N bond strength in hydrazine is 62.8 (ca. 65.4 kcal/mol in experiment[34]), so the two NH_2 radicals can recombine producing H_2NNH_2 without an entrance barrier and with high exothermicity. The energized hydrazine molecule can lose molecular hydrogen through a 1,1-H_2 elimination producing NNH_2 via TS3a. The barrier is 73.7 kcal/mol with respect to hydrazine but only 10.9 kcal/mol relative to the $NH_2 + NH_2$ reactants. Therefore, the 19.8 kcal/mol exothermic $NH_2 + NH_2 \rightarrow H_2NNH_2 \rightarrow NNH_2 + H_2$ reaction can occur at moderately elevated temperatures. On the other hand, energized hydrazine can also isomerize to $HNNH_3$ via TS4 lying 2.3 kcal/mol below the reactants and then dissociate without an exit barrier to $NH_3 + NH$. The $NH_2 + NH_2 \rightarrow H_2NNH_2 \rightarrow HNNH_3 \rightarrow NH_3 + NH(^3\Sigma^-)$ reaction is overall 14.3 kcal/mol exothermic but spin-forbidden, and the reaction leading to $NH_3 + NH$-($a^1\Delta$) is spin-allowed but 21.6 kcal/mol endothermic.

3.4. Why Are 1,1-H_2 Additions More Favorable Than 1,2-H_2 Additions? In order to break the H−H bond when molecular hydrogen approaches the N_2, N_2H_2, or N_2H_4 molecules, electron density has to be transferred to the antibonding σ_u molecular orbital (MO) of H_2. Therefore, the electron-donating occupied MO should be able to interact with the vacant σ_u MO. In the $N_2 + H_2$ reaction, molecular hydrogen can attack N_2 perpendicularly (1,1-addition) or parallel (1,2-addition) with respect to the N−N bond. As illustrated in Figure 5, the perpendicular approach via TS1a provides a much better overlap of the π MO of molecular nitrogen with the σ_u MO of H_2 than the nearly parallel approach via TS1b. Transition state TS3c for the 1,1-H_2 addition to *trans*-HNNH is similar to TS1a: a hydrogen molecule approaches in a plane perpendicular to the HNNH

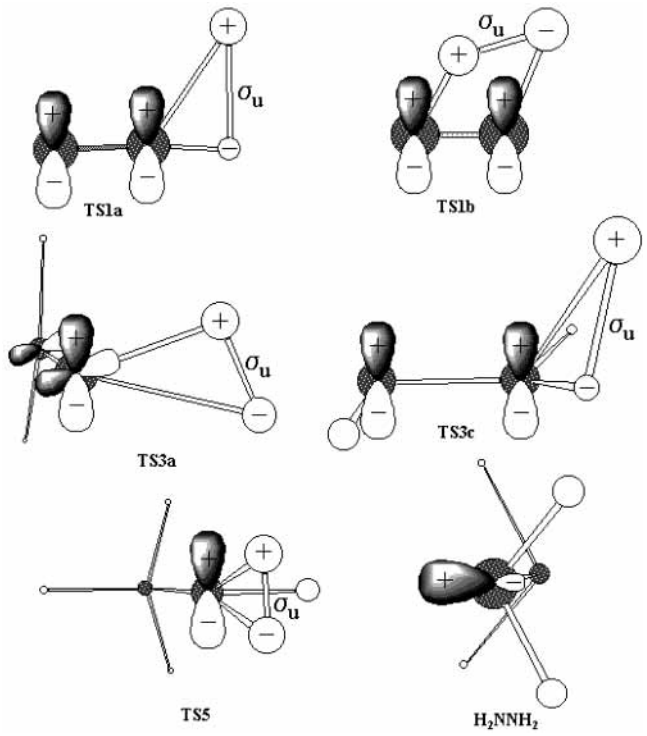

Figure 5. Schematic representation of molecular orbitals in various transition states donating electron density to the σ_u MO of H_2 during addition of molecular hydrogen to N_2, N_2H_2, and N_2H_4.

molecular plane so that the σ_u MO of H_2 can interact with the π-bonding MO of diazene. Again, a nearly parallel approach leading to the 1,2-H_2 addition via TS3b is much less favorable in terms of the orbital overlap and therefore exhibits a much higher barrier.

In the $NNH_2 + H_2$ and $HNNH_3 + H_2$ reactions, the orbitals which donate electron density to the σ_u MO of H_2 are p-orbitals containing a lone pair on the nitrogen atom. In this case, the maximal overlap is achieved when H_2 attacks NNH_2 or $HNNH_3$ parallel to these p-orbitals. Such an arrangement is most clearly seen in TS5. In TS3a, the σ_u MO can additionally interact with the π MO of NNH_2 and molecular hydrogen slightly deviates from the parallel position. The overlap of the hydrogen σ_u MO with a p-orbital of the nitrogen lone pair can be more efficient than with a π N−N bonding orbital because for the former case the electron density is mostly localized in the vicinity of the attacked nitrogen atom, whereas in the latter case the electron density is largely contained between two nitrogens, farther from the approaching H_2 molecule. As a result, the barriers at TS3a and TS5 are significantly lower than those at TS1a and TS3c. In the $H_2NNH_2 + H_2$ reaction, molecular hydrogen has to attack either the σ N−N MO or a lone pair of one of the nitrogens. The approach parallel to the N−N bond does not provide any overlap of the σ_u orbital with these MOs and the perpendicular approach (parallel to the lone pair) is sterically unfavorable. Hence, the H_2 addition cannot occur and we were not able to locate the corresponding transition state.

3.5. 2 *cis*-HNNH → $N_2 + N_2H_4$ Reaction. The second stage of nitrogen hydrogenation, the formation of N_2H_4, can be facilitated by the self-reaction of diazene. As was suggested by McKee et al.,[40] two *cis*-HNNH molecules can form a weak $N_2H_2 \cdot N_2H_2$ complex without an entrance barrier stabilized by 4.1 kcal/mol relative to the reactants. The complex decomposes to yield N_2 and hydrazine[40] via transition state TS7 by a concerted transfer of two hydrogen atoms. The 2 *cis*-HNNH → $N_2 + N_2H_4$ reaction is highly exothermic (by 76.9 kcal/mol), and the transition state TS7 demonstrates an early character, with two breaking N−H bonds only ∼4% longer than those in *cis*-diazene and two forming N−H bonds that are still ∼72% longer than those in hydrazine. The barrier is low, only 3.5 kcal/mol with respect to the complex, and TS7 lies 0.6 kcal/mol below the initial reactants. This indicates that if two *cis*-HNNH molecules approach each other, they will spontaneously form $N_2 + H_2NNH_2$.

3.6. Free Radical Chain Reaction Mechanism. The calculated barrier for the $N_2 + H_2 \rightarrow NNH_2$ reaction, 125.2 kcal/mol, is above the dissociation energy of H_2, 103.3 kcal/mol.[34] This suggests that reactions involving H radicals, $N_2 + H \rightarrow N_2H$ and subsequent chain reactions, may be involved in uncatalyzed nitrogen hydrogenation. Therefore, we have additionally investigated the following free radical chain reaction mechanism:

$$N_2 + H \rightarrow N_2H$$

$$N_2H + H_2 \rightarrow HNNH + H$$

$$HNNH + H \rightarrow N_2H_3$$

$$N_2H_3 + H_2 \rightarrow H_2NNH_2 + H$$

$$H_2NNH_2 + H \rightarrow NH_2 + NH_3$$

$$NH_2 + H_2 \rightarrow NH_3 + H$$

$$\text{net:} \quad N_2 + 3H_2 \rightarrow 2NH_3$$

The $N_2 + H \rightarrow N_2H$ reaction as well as the reverse reaction of the H atom loss in N_2H are believed to play a critical role in the thermal De-NO_x process[41−43] and were therefore investigated in detail earlier.[14−17] Our calculations (see Figures 3 and 4 and Table 1) show that the forward reaction is 11.4 kcal/mol endothermic and exhibits a barrier of 17.1 kcal/mol at transition state TS8. The classical barrier height and the classical exothermicity of the reverse reaction obtained at the G2M(MP2) level of theory are 10.3 and 4.5 kcal/mol. These values are in close agreement with the best estimates made by Schaefer and co-workers, 10.0 ± 1.0 and 3.8 ± 0.5 kcal/mol,[17] respectively, obtained on the basis of their CCSD(T)/aug-cc-pvqz calculations, and with earlier results by Walch and co-workers.[14−16]

The hydrogen abstraction $N_2H + H_2 \rightarrow$ *trans*-HNNH + H reaction has a higher endothermicity of 37.5 kcal/mol and proceeds via transition state TS9 with a barrier of 41.6 kcal/mol. TS9 depicts a typical geometry for an H abstraction transition state with a nearly linear N−H−H fragment. The breaking H−H bond is stretched by 36% to 1.012 Å, while the forming N−H is 15% longer than the bond in *trans*-diazene. This indicates a late character of the transition state, in line with the fact that the reaction is endothermic. The reverse reaction has a low barrier of 4.1 kcal/mol and is therefore expected to be fast. H + *trans*-HNNH → $N_2H + H_2$ has been investigated earlier by Chuang and Truhlar,[44] who obtained values of 4.3 and 37.4 kcal/mol for the reaction barrier and exothermicity, respectively, employing MRCI//CASSCF/cc-pvtz calculations. Our G2M(MP2) energies as well as the optimized geometry of TS9 are very similar to the results of Chuang and Truhlar.

A transition state search for hydrogen addition to diazene gives TS10 and IRC calculations showing that this transition state connects N_2H_3 with *cis*-HNNH + H. The H addition reaction is found to be highly exothermic, by 47.2 kcal/mol, and to exhibit a low barrier of 6.4 kcal/mol. Accordingly, TS10

has an early character with the forming N−H bond as long as 1.684 Å (compare to 1.357 Å in a late TS8 for endothermic H addition to N_2). The barrier for hydrogen addition to *cis*-HNNH is slightly higher than the barrier for H abstraction from *trans*-HNNH producing $N_2H + H_2$.

The N_2H_3 radical can in turn react with molecular hydrogen through the H abstraction mechanism producing $N_2H_4 + H$. This reaction is less endothermic (23.9 kcal/mol) than $N_2H + H_2 \rightarrow$ *trans*-HNNH + H and the barrier calculated at TS11 is lower, 29.1 kcal/mol. The geometries of the two H abstraction transition states, TS9 and TS11, are rather similar. The barrier in the reverse direction, $N_2H_4 + H \rightarrow N_2H_3 + H_2$, is low, 5.2 kcal/mol. The H atom can also add to the hydrazine molecule, but since a N_2H_5 species does not exist, this process can be better described as an exchange reaction. Two exchange mechanisms are possible, $N_2H_4 + H \rightarrow NH_2 + NH_3$ and $N_2H_4 + H \rightarrow N_2H_4 + H$. In the former, a new N−H bond is formed and the N−N bond is broken, while in the latter the attacking H atom kicks out one of the hydrogens of N_2H_4. The $N_2H_4 + H \rightarrow NH_2 + NH_3$ reaction is 43.8 kcal/mol exothermic (41.3 kcal/mol in experiment[34]) and proceeds via an early transition state TS12 where the forming N−H bond is 34% longer than the bond in NH_3 and the breaking N−N bond is elongated by 10%. On the other hand, the H exchange reaction occurring through TS13 is degenerate and thermoneutral and the coming and going hydrogen atoms are located symmetrically in the transition state. The H-for-NH_2 exchange reaction depicts a lower barrier, 10.7 kcal/mol, than that for the H-for-H exchange, 17.9 kcal/mol. Nevertheless, the barrier for $N_2H_4 + H \rightarrow NH_2 + NH_3$ is 5.5 kcal/mol higher than the barrier for the H abstraction reaction leading to $N_2H_3 + H_2$. Finally, NH_2 can abstract a hydrogen atom from H_2 producing $NH_3 + H$. This reaction has been studied in great detail both experimentally and theoretically.[18,19] We just recall here that the G2M calculated barrier is 13.6 kcal/mol, but in order to reproduce experimental reaction rate constants, it had to be adjusted to 10.6 kcal/mol.[19]

Overall, the free radical chain reaction mechanism of nitrogen hydrogenation shows much lower barriers and should be significantly more efficient than the molecular mechanism. One can say that the $N_2 + 3H_2 \rightarrow 2NH_3$ reaction is catalyzed in the presence of H radicals. The highest barrier along the reaction pathway, 41.6 kcal/mol, is found for the $N_2H + H_2 \rightarrow$ HNNH + H hydrogen abstraction step. The chain reactions can be terminated by barrierless H atom additions to N_2H and N_2H_3 where the strengths of the forming N−H bonds are computed as 63.6 and 77.1 kcal/mol, respectively (see Figure 3).

3.7. Reaction Rate Constants and Equilibrium Constants. Using the calculated reaction energetics and molecular parameters, one can employ transition state theory to compute rate constants at various temperatures. For the reactions which have a unimolecular character in the forward or reverse direction, the TST rates correspond to the high-pressure limit, while their pressure dependence can be evaluated using RRKM theory, which is beyond the scope of this paper. Here, reaction rate constants were estimated according to the following formula:[45]

$$k = \left(\frac{RT}{p^{\ominus}}\right)^{-\Delta n^{\ddagger}} \frac{k_B T}{h} e^{-\Delta G_0^{\ddagger}/RT}$$

where R is the Rydberg constant, k_B is the Boltzmann constant, h is the Planck constant, T and $p^{\ominus}$ are the temperature and the standard pressure, respectively, $\Delta n^{\ddagger}$ is the change of the number of moles from reactants to the transition state, and $\Delta G_0^{\ddagger}$ is the change of the Gibbs free energy from reactants to the transition state. Tunneling corrections (Q_{tun}) to the TST rate constants were computed using the Wigner formula[46]

$$Q_{tun} = 1 - \frac{1}{24}\left(\frac{h\nu_S}{k_B T}\right)^2 (1 + k_B T/E_0)$$

where ν_S is the transition state imaginary frequency and E_0 is the barrier height including ZPE correction. Equilibrium constants were computed using ab initio energies and molecular structural parameters as follows:

$$K_{eq} = \left(\frac{RT}{p^{\ominus} N_A}\right)^{-\Delta n} e^{-\Delta G_0/RT}$$

where N_A is the Avogadro constant, Δn is the change of the number of moles in the reaction, and ΔG_0 is the Gibbs free energy of the reaction.

The calculated rate constants in forward and reverse directions as well as equilibrium constants for various reactions of molecular and chain radical mechanisms of nitrogen hydrogenation are collected in Table S1 of the Supporting Information. Table 4 shows least-squares fitted two- and three-parameter expressions for various reaction rates. These rate constants can be utilized for kinetic modeling of chemical reactions involving nitrogen- and hydrogen-containing species. As seen in Table 4, preexponential factors for unimolecular reactions lie in the range of $(0.26-2.54) \times 10^{14}$ s^{-1} but in general are close to 10^{14} s^{-1}. For bimolecular reactions, preexponential factors vary in a broader interval between 2.9×10^{-13} cm^3 $molecule^{-1}$ s^{-1} ($NH_2 + NH_3 \rightarrow N_2H_4 + H$) and 2.5×10^{-10} cm^3 $molecule^{-1}$ s^{-1} ($HNNH_3 + H_2 \rightarrow 2NH_3$). Activation energies in the two-parameter expressions are similar to the calculated reaction barriers. The rates of bimolecular reactions are better fitted with three-parameter $AT^B \exp(-C/T)$ expressions, especially at high temperatures. Some comparisons can be made for rate constants of the *trans*-HNNH + H → $N_2H + H_2$ reaction, for which Chuang and Truhlar carried out direct dynamics calculations with inclusion of multidimensional tunneling effects.[44] The rates in cm^3 $molecule^{-1}$ s^{-1} at 300, 600, 1500, and 3000 K, respectively, are the following: 2.8×10^{-13} (present calculations) vs 6.8×10^{-13} (Chuang and Truhlar[44]), 3.5×10^{-12} vs 3.5×10^{-12}, 3.5×10^{-11} vs 3.4×10^{-11}, and 1.4×10^{-10} vs 2.0×10^{-10}. Thus, the results closely agree except for the low 300 K temperature, where tunneling plays a critical role and sophisticated methods applied by Chuang and Truhlar to obtain the tunneling probabilities should be more reliable than the simple Wigner correction.

4. Conclusions

We have carried out ab initio G2M(MP2)//MP2/6-31G** calculations in order to investigate the molecular and radical chain reaction mechanisms of uncatalyzed hydrogenation of the nitrogen molecule through sequential addition of three H_2 molecules producing two molecules of ammonia. The results show that all reaction steps are slow owing to high barriers for the molecular hydrogen additions. The three-center 1,1-H_2 additions (via TS1a, TS3a, TS3c, and TS4) are clearly preferable as compared to the four-center 1,2-additions (TS1b and TS3b). The most favorable reaction pathways in the molecular mechanism involve the steps $N_2 + H_2 \rightarrow$ TS1a → NNH_2, $NNH_2 + H_2 \rightarrow$ TS3a → H_2NNH_2, $H_2NNH_2 \rightarrow$ TS4 → $HNNH_3$, and $HNNH_3 + H_2 \rightarrow$ TS5 → $NH_3 + NH_3$, with the barriers calculated as 125.2, 30.7, 60.5, and 24.6 kcal/mol, respectively.

TABLE 4: Fitted Two- and Three-Parameter Expressions for Rate Constants of Various Reactions

reaction	expression	units, temp range
$NNH_2 \rightarrow N_2 + H_2$	$2.54 \times 10^{14} \exp(-52785/RT)$	s^{-1}, 300−5000 K
$NNH_2 \rightarrow$ *trans*-HNNH	$1.33 \times 10^{14} \exp(-46931/RT)$	s^{-1}, 300−5000 K
trans-HNNH $\rightarrow NNH_2$	$1.37 \times 10^{14} \exp(-71613/RT)$	s^{-1}, 300−5000 K
trans-HNNH $\rightarrow$ *cis*-HNNH	$6.39 \times 10^{13} \exp(-49818/RT)$	s^{-1}, 300−5000 K
cis-HNNH $\rightarrow$ *trans*-HNNH	$5.90 \times 10^{13} \exp(-44964/RT)$	s^{-1}, 300−5000 K
$NNH_2 + H_2 \rightarrow N_2H_4$	$3.47 \times 10^{-19} T^{2.27} \exp(-13814/T)$	cm^3 molecule^{-1} s^{-1}, 300−5000 K
	$6.14 \times 10^{-12} \exp(-29783/RT)$	cm^3 molecule^{-1} s^{-1}, 300−1000 K
$N_2H_4 \rightarrow NNH_2 + H_2$	$1.38 \times 10^{14} \exp(-74911/RT)$	s^{-1}, 300−5000 K
trans-HNNH + $H_2 \rightarrow HNNH_3$	$3.68 \times 10^{-19} T^{2.15} \exp(-27392/T)$	cm^3 molecule^{-1} s^{-1}, 300−5000 K
	$2.92 \times 10^{-12} \exp(-56659/RT)$	cm^3 molecule^{-1} s^{-1}, 300−1000 K
$HNNH_3 \rightarrow$ *trans*-HNNH + H_2	$2.58 \times 10^{13} \exp(-35492/RT)$	s^{-1}, 300−5000 K
$N_2H_4 \rightarrow HNNH_3$	$9.17 \times 10^{13} \exp(-61331/RT)$	s^{-1}, 300−5000 K
$HNNH_3 \rightarrow N_2H_4$	$9.60 \times 10^{13} \exp(-20589/RT)$	s^{-1}, 300−5000 K
$HNNH_3 + H_2 \rightarrow 2NH_3$	$1.50 \times 10^{-18} T^{2.59} \exp(-11532/T)$	cm^3 molecule^{-1} s^{-1}, 300−5000 K
	$2.53 \times 10^{-10} \exp(-25473/RT)$	cm^3 molecule^{-1} s^{-1}, 300−1000 K
$N_2 + H \rightarrow N_2H$	$2.14 \times 10^{-14} T^{0.88} \exp(-7965/T)$	cm^3 molecule^{-1} s^{-1}, 300−5000 K
	$1.47 \times 10^{-10} \exp(-16216/RT)$	cm^3 molecule^{-1} s^{-1}, 300−1000 K
$N_2H \rightarrow N_2 + H$	$3.51 \times 10^{11} T^{0.66} \exp(-2531/T)$	s^{-1}, 300−5000 K
	$4.11 \times 10^{13} \exp(-5630/RT)$	s^{-1}, 300−1000 K
$N_2H + H_2 \rightarrow$ *trans*-HNNH + H	$1.11 \times 10^{-19} T^{2.33} \exp(-18939/T)$	cm^3 molecule^{-1} s^{-1}, 300−5000 K
	$3.29 \times 10^{-12} \exp(-40083/RT)$	cm^3 molecule^{-1} s^{-1}, 300−1000 K
trans-HNNH + H $\rightarrow N_2H + H_2$	$5.98 \times 10^{-16} T^{1.58} \exp(-864/T)$	cm^3 molecule^{-1} s^{-1}, 300−5000 K
	$6.91 \times 10^{-11} \exp(-3350/RT)$	cm^3 molecule^{-1} s^{-1}, 300−1000 K
cis-HNNH + H $\rightarrow N_2H_3$	$1.12 \times 10^{-15} T^{1.42} \exp(-2231/T)$	cm^3 molecule^{-1} s^{-1}, 300−5000 K
	$3.74 \times 10^{-11} \exp(-5882/RT)$	cm^3 molecule^{-1} s^{-1}, 300−1000 K
$N_2H_3 \rightarrow$ *cis*-HNNH + H	$7.95 \times 10^{13} \exp(-54569/RT)$	s^{-1}, 300−5000 K
$N_2H_3 + H_2 \rightarrow N_2H_4 + H$	$7.13 \times 10^{-20} T^{2.43} \exp(-12785/T)$	cm^3 molecule^{-1} s^{-1}, 300−5000 K
	$4.54 \times 10^{-12} \exp(-27947/RT)$	cm^3 molecule^{-1} s^{-1}, 300−1000 K
$N_2H_4 + H \rightarrow N_2H_3 + H_2$	$7.53 \times 10^{-17} T^{1.80} \exp(-1315/T)$	cm^3 molecule^{-1} s^{-1}, 300−5000 K
	$4.16 \times 10^{-11} \exp(-4447/RT)$	cm^3 molecule^{-1} s^{-1}, 300−1000 K
$N_2H_4 + H \rightarrow NH_2 + NH_3$	$3.84 \times 10^{-16} T^{1.42} \exp(-4128/T)$	cm^3 molecule^{-1} s^{-1}, 300−5000 K
	$1.37 \times 10^{-11} \exp(-9675/RT)$	cm^3 molecule^{-1} s^{-1}, 300−1000 K
$NH_2 + NH_3 \rightarrow N_2H_4 + H$	$3.16 \times 10^{-23} T^{3.11} \exp(-25218/T)$	cm^3 molecule^{-1} s^{-1}, 300−5000 K
	$2.87 \times 10^{-13} \exp(-53311/RT)$	cm^3 molecule^{-1} s^{-1}, 300−1000 K
$NH_2 + H_2 \rightarrow NH_3 + H$[a]	$5.37 \times 10^{-19} T^{2.23} \exp(-3607/T)$	cm^3 molecule^{-1} s^{-1}, 300−5000 K

[a] From ref 19.

With respect to the most stable isomers of diazene and hydrazine, the highest barriers on the reaction pathways for the addition of the first, second, and third H_2 molecules are 125.2, 57.5, and 65.5 kcal/mol, respectively. Therefore, the addition of the first molecular hydrogen is the rate-determining stage of nitrogen hydrogenation. The formation of hydrazine can be facilitated by a spontaneous reaction of two *cis*-HNNH molecules by the dihydrogen transfer mechanism. The radical chain mechanism includes the sequential reactions $N_2 + H \rightarrow N_2H$, $N_2H + H_2 \rightarrow HNNH + H$, $HNNH + H \rightarrow N_2H_3$, $N_2H_3 + H_2 \rightarrow H_2NNH_2 + H$, $H_2NNH_2 + H \rightarrow NH_2 + NH_3$, and $NH_2 + H_2 \rightarrow NH_3 + H$, with the barriers of 17.1, 41.6, 6.4, 29.1, 10.7, and 10.6 kcal/mol, respectively. Thus, nitrogen hydrogenation can be catalyzed by H atoms and the slowest reaction step in this case is found to be the hydrogen abstraction from H_2 by N_2H. Although it is costly to break the H−H bond to form H atoms from molecular hydrogen, the radical chain mechanism could be initiated with irradiation of H_2 by light or in the presence of a catalyst able to supply H atoms to the reaction system.

The reaction of two imino radicals, $NH(^3\Sigma^-)$, is predicted to be fast and to produce $N_2 + H_2$ with high exothermicity. On the other hand, the reaction of two amino radicals, $2NH_2(^2B_1) \rightarrow H_2NNH_2 \rightarrow$ TS3a $\rightarrow NNH_2 + H_2$, is calculated to be 19.8 kcal/mol exothermic and to exhibit a barrier of 10.9 kcal/mol relative to the reactants. Another reaction channel, $2NH_2(^2B_1) \rightarrow H_2NNH_2 \rightarrow$ TS4 $\rightarrow HNNH_3 \rightarrow NH_3 + NH(^3\Sigma^-)$, exothermic by 14.3 kcal/mol, does not have to go via a transition state lying above the reactants but is spin-forbidden.

Acknowledgment. Funding from Tamkang University was used to buy the computer equipment used in part of this investigation. A partial support from Academia Sinica and from the National Science Council of Taiwan, R.O.C., is also appreciated.

Supporting Information Available: Calculated rate constants in the forward and reverse directions and equilibrium constants for various reactions involved in nitrogen hydrogenation in the 300−5000 K temperature range. This material is available free of charge via the Internet at http://pubs.acs.org.

References and Notes

(1) Büchel, H.; Moretto, H.-H.; Woditsch, P. *Industrielle Anorganische Chemie*; Wiley/VCH: Weinheim, 1999; Vol. 3.
(2) McBryde, A. E. In *Nobel Laureates in Chemistry*; James, L. K., Ed.; American Chemical Society and Chemical Heritage Foundation: Washington, D.C., 1993.
(3) Kim, J.; Rees, D. C. *Biochemistry* **1994**, *33*, 389.
(4) Howard, B.; Rees, D. C. *Chem. Rev.* **1996**, *96*, 2965.
(5) Whitelegg, D.; Woolley, R. G. *J. Mol. Struct. (THEOCHEM)* **1990**, *209*, 23.
(6) Andzelm, J.; Sosa, C.; Eades, R. A. *J. Phys. Chem.* **1993**, *97*, 4664.
(7) Smith, B. *J. Phys. Chem.* **1993**, *97*, 10513.
(8) Andzelm, J.; Baker, J.; Scheiner, A.; Wrinn, M. *Int. J. Quantum Chem.* **1995**, *56*, 733.
(9) Curtiss, L. A.; Raghavachari, K.; Redfern, P. C.; Rassolov, V.; Pople, J. A. *J. Chem. Phys.* **1998**, *109*, 7764.
(10) Sekušak, S.; Frenking, G. *J. Mol. Struct. (THEOCHEM)* **2001**, *541*, 17.
(11) Strobel, D. F. *Int. Rev. Phys. Chem.* **1983**, *3*, 145.
(12) Lyon, R. K. *Int. J. Chem. Kinet.* **1976**, *8*, 318; U.S. Patent 3,900,554.
(13) Perry, R. A.; Siebers, D. L. *Nature* **1986**, *324*, 657.
(14) Walch, S. P. *J. Chem. Phys.* **1990**, *93*, 2384.

(15) Koizumi, H.; Schatz, G. C.; Walch, S. P. *J. Chem. Phys.* **1991**, *95*, 4130.
(16) Walch, S. P.; Partridge, H *Chem. Phys. Lett.* **1995**, *233*, 331.
(17) Gu, J.; Xie, Y.; Schaefer, H. F., III. *J. Chem. Phys.* **1998**, *108*, 8029.
(18) Mebel, A. M.; Moskaleva, L. V.; Lin, M. C. In *N-centered Radicals*; Alfassi, Z. B., Ed.; Wiley: New York, 1998; p 467, and references therein.
(19) Mebel, A. M.; Moskaleva, L. V.; Lin, M. C. *J. Mol. Struct. (THEOCHEM)* **1999**, *461*−*462*, 223.
(20) Hehre, W. J.; Radom, L.; Schleyer, P. v. R.; Pople, J. A. *Ab Initio Molecular Orbital Theory*; Wiley: New York, 1986.
(21) Gonzales, C.; Schlegel, H. B. *J. Chem. Phys.* **1989**, *90*, 2154.
(22) Scott, A. P.; Radom, L. *J. Phys. Chem.* **1996**, *100*, 16502.
(23) Mebel, A. M.; Morokuma, K.; Lin, M. C. *J. Chem. Phys.* **1995**, *103*, 7414.
(24) Curtiss, L. A.; Raghavachari, K.; Trucks, G. W.; Pople, J. A. *J. Chem. Phys.* **1991**, *94*, 7221. (b) Pople, J. A.; Head-Gordon, M.; Fox, D. J.; Raghavachari, K.; Curtiss, L. A. *J. Chem. Phys.* **1989**, *90*, 5622. (c) Curtiss, L. A.; Jones, C.; Trucks, G. W.; Raghavachari, K.; Pople, J. A. *J. Chem. Phys.* **1990**, *93*, 2537. (d) Curtiss, L. A.; Raghavachari, K.; Pople, J. A. *J. Chem. Phys.* **1993**, *98*, 5523.
(25) Purvis, G. D.; Bartlett, R. J. *J. Chem. Phys.* **1982**, *76*, 1910.
(26) Frisch, M. J.; Trucks, G. W.; Schlegel, H. B.; Scuseria, G. E.; Robb, M. A.; Cheeseman, J. R.; Zakrzewski, V. G.; Montgomery, J. A., Jr.; Stratmann, R. E.; Burant, J. C.; Dapprich, S.; Millam, J. M.; Daniels, A. D.; Kudin, K. N.; Strain, M. C.; Farkas, O.; Tomasi, J.; Barone, V.; Cossi, M.; Cammi, R.; Mennucci, B.; Pomelli, C.; Adamo, C.; Clifford, S.; Ochterski, J.; Petersson, G. A.; Ayala, P. Y.; Cui, Q.; Morokuma, K.; Malick, D. K.; Rabuck, A. D.; Raghavachari, K.; Foresman, J. B.; Cioslowski, J.; Ortiz, J. V.; Baboul, A. G.; Stefanov, B. B.; Liu, G.; Liashenko, A.; Piskorz, P.; Komaromi, I.; Gomperts, R.; Martin, R. L.; Fox, D. J.; Keith, T.; Al-Laham, M. A.; Peng, C. Y.; Nanayakkara, A.; Gonzalez, C.; Challacombe, M.; Gill, P. M. W.; Johnson, B.; Chen, W.; Wong, M. W.; Andres, J. L.; Head-Gordon, M.; Replogle, E. S.; Pople, J. A. *Gaussian 98*, revision A.7; Gaussian, Inc.: Pittsburgh, PA, 1998.
(27) Rozenbaum, V. M.; Mebel, A. M.; Lin, S. H. *Mol. Phys.* **2001**, *99*, 1883.
(28) DeFrees, D. J.; Levi, B. A.; Pollack, S. K.; Binkley, J. S.; Pople, J. A. *J. Am. Chem. Soc.* **1979**, *101*, 4085.
(29) Casewit, C. J.; Goddard, W. A., III. *J. Am. Chem. Soc.* **1980**, *102*, 4057.
(30) Pople, J. A.; Raghavachari, K.; Frisch, J. J.; Binkley, J. S.; Schleyer, P. v. R. *J. Am. Chem. Soc.* **1983**, *105*, 6389.
(31) Jensen, H. J. A.; Jorgensen, P.; Helgaker, T. *J. Am. Chem. Soc.* **1987**, *109*, 2895.
(32) Walch, S. P. *J. Chem. Phys.* **1989**, *91*, 389.
(33) Brandemark, U.; Siegbahn, P. E. M. *Theor. Chim. Acta* **1984**, *66*, 217.
(34) Experimental heats of formation of various species, $\Delta H_f(0\ \mathrm{K})$, are taken from references cited in refs 17 and 18.
(35) Biehl, H.; Stuhl, F. *J. Chem. Phys.* **1994**, *100*, 141.
(36) *NIST Chemistry Webbook*; NIST Standard Reference Data Base Number 69, February 2000 Release (http://webbook.nist.gov/chemistry/).
(37) Werner, H.-J.; Knowles, P. J. *J. Chem. Phys.* **1985**, *82*, 5053. (b) Knowles, P. J.; Werner, H.-J. *Chem. Phys. Lett.* **1985**, *115*, 259.
(38) Werner, H.-J.; Knowles, P. J. *J. Chem. Phys.* **1988**, *89*, 5803. (b) Knowles, P. J.; Werner, H.-J. *Chem. Phys. Lett.* **1988**, *145*, 514.
(39) MOLPRO is a package of ab initio programs written by H.-J. Werner and P. J. Knowles with contributions from J. Almlöf, R. D. Amos, M. J. O. Deegan, S. T. Elbert, C. Hampel, W. Meyer, K. Peterson, R. Pitzer, A. J. Stone, P. R. Taylor, and R. Lindh.
(40) McKee, M. L.; Squillacote, M. E.; Stanbury, D. M. *J. Phys. Chem.* **1992**, *96*, 6, 3266.
(41) Miller, C. A.; Bowman, C. T. *Prog. Energy Combust. Sci.* **1989**, *15*, 287.
(42) Miller, J. A.; Kee, R. J.; Westbrook. *Annu. Rev. Phys. Chem.* **1990**, *41*, 345.
(43) Miller, J. A.; Glarborg, P. *Springer Series in Chemical Physics*; Springer: Berlin, 1996; Vol. 61, p 318.
(44) Chuang, Y.-Y.; Truhlar, D. G. *J. Phys. Chem. A* **1997**, *101*, 3808.
(45) Glasstone, S.; Laidler, K. J.; Eyring, H. *The Theory of Rate Processes*; McGraw-Hill: New York, 1941.
(46) Steinfield, J.; Francisco, J.; Hase, W. *Chemical Kinetics and Dynamics*; Prentice-Hall: Englewood Cliffs, NJ, 1989.